Environmental Monitoring and Evaluation of Flash Floods Using Remote-Sensing and GIS Techniques

Noha Donia

Abstract

Egypt receives very little rainfall apart from on its coastal areas where average annual rainfall is 50–250 mm on its west coast and 50–150 mm on its east coast—rainfall increases from west to east. As a result of such low levels of rainfall Egypt might be considered safe from flooding. However, such an assumption would be dangerous because Egypt is exposed to high rainfall rates every 100 years. Therefore, studies must be carried out on all Egypt's basins to study their characteristics and calculate probable flood volumes for such events, thereby allowing the provision of flood protection. As traditional methods of flood response are put under pressure by dynamic changes experienced in Egypt, this chapter presents a model for the application of advanced technologies such as remoyte-sensimg and GIS techniques capable of identifying and monitoring flash floods and watershed delineation and flood estimation in different areas in Egypt.

Keywords

Flash floods • GIS • Remote sensing • Egypt • Model • Rainfall

1 Introduction

A flood is generally defined as the location of a flow of water; geologically it is the flow of water over the ground. Floods are governed by a number of factors, the most important being rainfall, evaporation, and leakage. Meteorologically, a flood is defined as the result of heavy rainfall —associated with the occurrence of sudden atmospheric instability over mountainous areas during the cold, winter season. The three major flood types are flash floods, rapid onset floods, and slow onset floods.

Flash floods result from heavy rain, dam breaks, or snowmelt. They occur over very short timeframes (2–6 h, sometimes in a matter of minutes). They can also be caused by intense rainfall from slow-moving thunderstorms. Flash floods are destructive and can be fatal—commonly taking people by surprise. Often they arrive with no warning, allowing no preparation, with impacts both swift and devastating.

Rapid Onset Floods take longer to develop than a flash flood and tends to last only for a day or two. Such floods can be managed by people but are very destructive.

Water bodies overflowing their banks cause slow onset floods. They are slow to develop but can last for days or weeks. They usually spread over many kilometers and tend to occur in flood plains (fields prone to flooding in low-lying areas). They bring with them disease and malnutrition as well as an increase in the number of snakebites—rising water levels drive animals into closer proximity to people.

Floods arguably represent the most devastating, widespread, and frequently occurring natural hazards globally. Flash floods are formed from excess rain falling on upstream watersheds, rapidly flowing downstream with great speed and force. Often, they are sudden and appear without warning. Therefore, such floods have considerable consequences, with damage becoming especially pronounced when water flows through human settlements and concentrations of infrastructure.

Remote sensing and geographic information systems (GIS) provide a wide range of tools for determining areas affected by flash floods and delineating watersheds. A GIS can be used to assemble information from different maps, aerial photographs, satellite images, and digital elevation

N. Donia (✉)
Department of Environmental Engineering, Institute of Environmental Studies and Research, Ain Shams University, Cairo, Egypt
e-mail: Noha.samir@iesr.asu.edu.eg

A. M. Negm (ed.), *Flash Floods in Egypt*, Advances in Science, Technology & Innovation,
https://doi.org/10.1007/978-3-030-29635-3_8

models (DEMs). Remote-sensing technology along with GIS has become the key tool for load hazard and risk maps for vulnerable areas. El Bastawesy et al. (2008, 2009, 2012) and Yousif et al. (2013) applied GIS and remote-sensing techniques for watershed delineation.

This chapter attempts to synthesize a database in a spatial framework to create a flood risk map using remote-sensing and GIS techniques. This study also focuses on the identification of factors affecting flash flood risk.

2 Methodology

A watershed is an area of land that contributes runoff water to a common point, it is a natural physiographic or ecological unit composed of interrelated parts and functions (Al-Jabari et al. 2009), determined by the topography of the land around it. Identifying a watershed is necessary to calculate runoff depth and volume; drainage networks are necessary for water-harvesting activities. In this study, drainage networks and watersheds are identified using a DEM and ArcGIS 10.1 software from Esri—an American company specializing in GIS. This represents the latest computer technology and can be used for processing and spatial analysis in 3D. It permits the processing and interpretation of enormous spatial and descriptive data and provides outputs in the form of maps and reports. The program can also be used to extract basin watersheds, drainage networks, stream order, flow, and direction, and other basin characteristics using ArcHydro, part of Arc Toolbox. The software is comprised of a collection of tools for basin analysis and hydrological applications (O'Callaghan and Mark 1984).

2.1 Watershed and Drainage Network Delineation Using a Geographic Information System

2.1.1 Digital Elevation Model

A DEM represents a 3D view of the Earth's terrain and has significant applications in science and other fields. DEMs depend on aerial images, global signature systems, and digital signage. They use either a geographic grid with spacing along parallels and meridians—in which case data spacing changes because of the curvature of the Earth—or they use a projected grid like Universal Transverse Mercator (UTM)—in which case the merging of datasets eventually becomes a problem because of the Earth's curvature. Small-scale DEMs generally use geographic grids, whereas large-scale DEMs can use either projected or geographic grids. The DEM used in this study was based on data from the Shuttle Radar Topography Mission (SRTM)—a space survey of Earth by NASA, the National Geospatial-Intelligence Agency (NGA), DLR (Germany's national aeronautics and space research center), and ISA providing radar data (wavelength of 56 mm) with 90-m spatial resolution (obtained from the United States Geological Survey website, http://www.usgs.gov.)

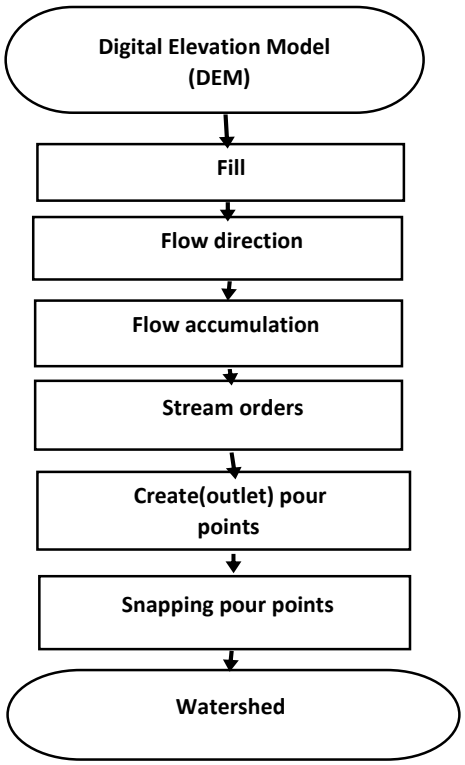

Fig. 1 Hydrological processing using ArcGis 10.1 software

The drainage network and watershed were delineated from DEM inputs (Jones 2002). The hydrological processing steps are shown in Fig. 1 and were completed using ArcGis 10.1 software in Arc Hydro in the main interface of Arc Toolbox (ESRI 2010).

STEP 1 Fill operation

This operation was used to remove all possible and abnormal values—either sink or peak errors—due to data with no resolution or a rounding of elevations to the nearest integer, to ensure proper watershed and stream delineation.

STEP 2 Flow direction

The flow direction for each well was determined using the ARCGIS grid processor. Additionally, the D-8 drainage model was used to derive flow directions between the central cell and its eight adjacent neighbors.

STEP 3 Flow accumulation

Cells with the greatest accumulated flow were determined and a network of high-flow cells created. Flow accumulation can be used to determine how much rain has fallen within a given watershed—flow accumulation output, representing the amount of rain flowing through each cell, was used to determine the drainage pattern (defined in terms of cumulative contribution counts for drained water into outlets).

STEP 4 Stream orders

The stream order of a watershed reflects the ability of a stream to erode and deposit sediment and is therefore linked to soil erosion and flooding. In this study, Strahler's method was used to identify and classify stream type based on tributary numbers.

STEP 5 Create outlet (pour) points

Pour point placement is an important step in the process of watershed delineation. Pour points should be positioned within an area of high flow accumulation to calculate total contributing water flow.

STEP 6 Snapping pour points

The Snap Pour Point tool snaps pour points created in Step 5 to the closest cell of high flow accumulation to account for any error during placement.

STEP 7 Watershed delineation

The watershed was delineated using a flow-direction raster.

2.1.2 The Main Morphometric Parameters of the Watershed and Drainage Networks

The area and perimeter of the watershed, the order of its streams, and the sum of stream lengths within drainage networks were calculated using ArcGIS 10.1 software.

Drainage density is an important factor related to geomorphology and hydrology. It reflects the method of surface water flow according to geology, gradient, plant cover, and the quantity and intensity of precipitation. Drainage density was calculated using the following equation:

$$LDD = SL/A$$

where SL is the sum of stream lengths; A is the area of the watershed (Rashash et al. 2015); and LDD the longitudinal drainage density.

2.1.3 Sub-watersheds

The main watershed was divided into sub-watersheds depending on land use/cover and the positions of cultivated areas between dykes through wadis to determine the effect of geomorphology on surface runoff, study the effect of spillway height on water distribution through wadis, and calculate the lost runoff volume to the sea.

2.2 Estimation of Surface Runoff

Water is one of the most important resources in arid and semi-arid regions and is essential to their development. Runoff estimation is especially helpful in areas lacking measuring stations (Al-Gamdi 1991). Surface runoff is the flow of precipitated water in a catchment area through a channel after all surface and sub-surface losses (Bansode and Patil 2014). In this study, an estimate of surface runoff was based on watershed characteristics, the natural components associated with land use/land cover, hydrological soil group (HSG), monthly rainfall, and antecedent moisture conditions using the Soil Conservation Service (SCS) curve number method and GIS. The runoff estimation methodology is shown in Fig. 2.

The SCS of the US Department of Agriculture developed the curve number (SCS-CN) method, also known as the Hydrologic Soil Cover Complex Method. This procedure has been used widely for runoff estimation. Rainfall amount and curve number are needed for this method and depend on the HSG of an area, land use, and hydrological conditions. Normally the SCS model computes direct runoff with the help of the following relationship:

$$S = (25400/CN) - 254$$

$$I_a = 0.2S$$

$$CN = \Sigma(CN_i times A_i)/A$$

$$Q = (P - I_a)^2/(P - I_a) + S$$

where:

- CN is the runoff curve number of a hydrological soil cover complex;
- S is the potential maximum retention of water by the soil (mm);
- I_a is the initial abstraction which represents all losses before runoff begins (mm);
- P is the total storm rainfall (mm);
- Q is the actual direct runoff (mm);
- CN_i is the curve number from $i = 1$ to the number of areas;

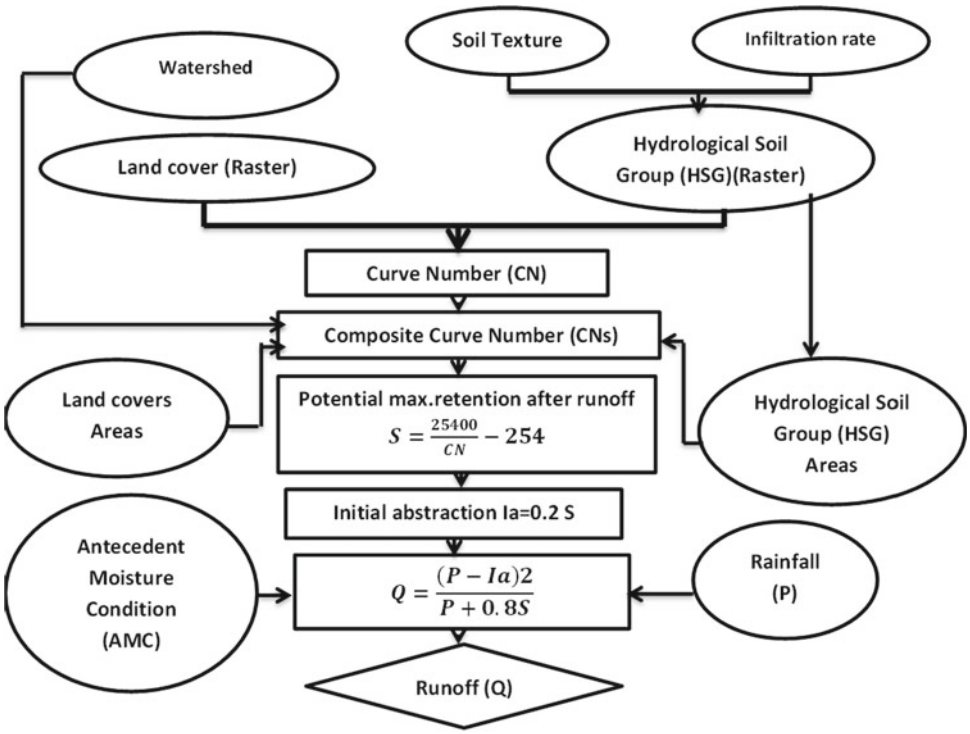

Fig. 2 Runoff estimation methodology

A_i is the area with curve number CNi (m^2); and
A is the total area of the watershed (m^2)

3 Study Areas

3.1 Wadi Firan

Wadi Firan is about 90 km east of Abou Redis, in the Sinai governorate. It includes 47 principal settlements and 22 secondary settlements and has a population of 7000. It contains many historical sites (Dir el Banat) and includes two churches (Nabi Mouus and Anba Dinamous). Monagat Mountain is 1 km west of Wadi Firan village. In addition, the region of Briga and the historical site of Nabtia are about 3 km from the village. Tahouna Mountain (the location of Alia Nabi Church and Actafious Church) is also nearby, as is Serbal Mountain—in the Agla Seil region—and the historical site of Nawawis. The area of Firan is illustrated in Fig. 3 and its geological map is provided in Fig. 4. The watershed model for the area, created using GIS, is shown in Fig. 5. Figures 6, 7, 8, and 9 show the results of a GIS analysis of the watershed.

3.2 Wadi Hashim

The area of Wadi Hashim is located about 50 km east of the city of Marsa Matrouh, bounded by latitudes 31°8′0″N and 31°9′0″N and longitudes 27°37′30″E and 27°38′30″E (Fig. 10). The drainage networks and watershed were extracted using ArcGIS 10.1 software (Fig. 10). The watershed was linked with an attribute table and its area calculated to be 3.305 km^2.

3.2.1 Land Use

The locations of different land use classes were determined during a field survey using GPS devices. Their boundaries were digitized using ArcGIS 10.1, attribute tables were assigned, and areas calculated (Table 1 and in Fig. 11).

The watershed was found to comprise three classes of land use with bare soil covering the greatest area (1.834 km^2, representing 55.5%) and cultivated land covering the least area (0.255 km^2, representing 7.7%).

3.2.2 Soil Texture

The particle size distribution of eight samples of soil from four sites, incorporating all land use types, was determined according to the United States Department of Agriculture (USDA) classification and soil textures were determined with the USDA soil texture triangle. The results are given in Table 2 and show that the soil texture of all samples is sandy loam.

3.2.3 Soil Infiltration Rate

Infiltration rates for soils, at the same sampling sites used to ascertain soil texture, were determined using a double-ring

Fig. 3 Study area

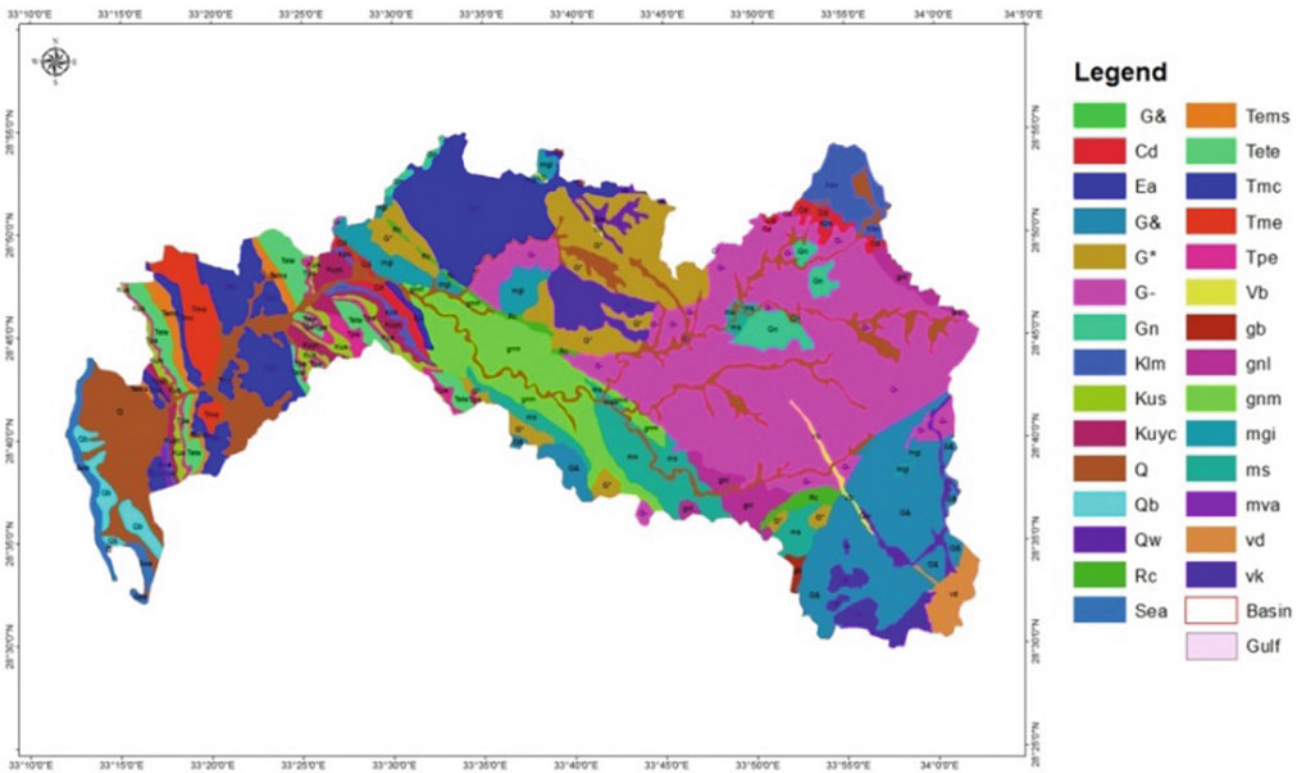

Fig. 4 Geological map of the study area

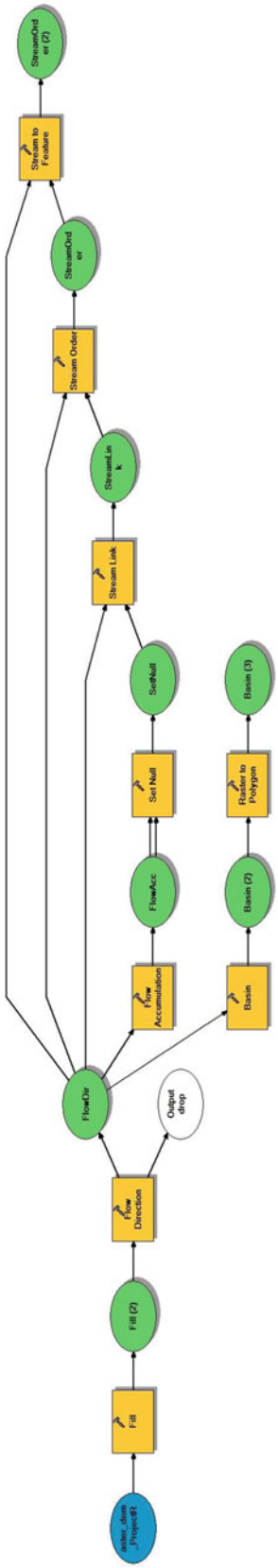

Fig. 5 Watershed model

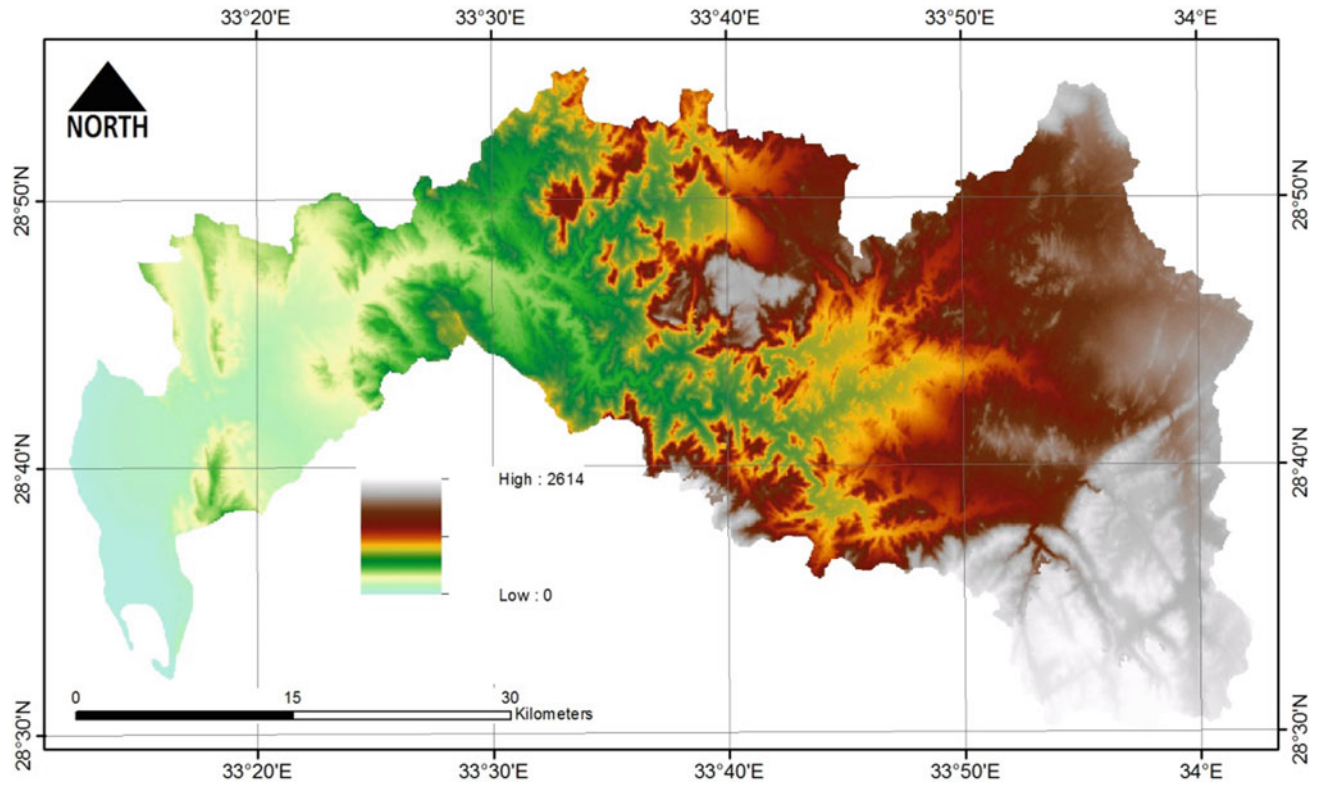

Fig. 6 DEM of the study area

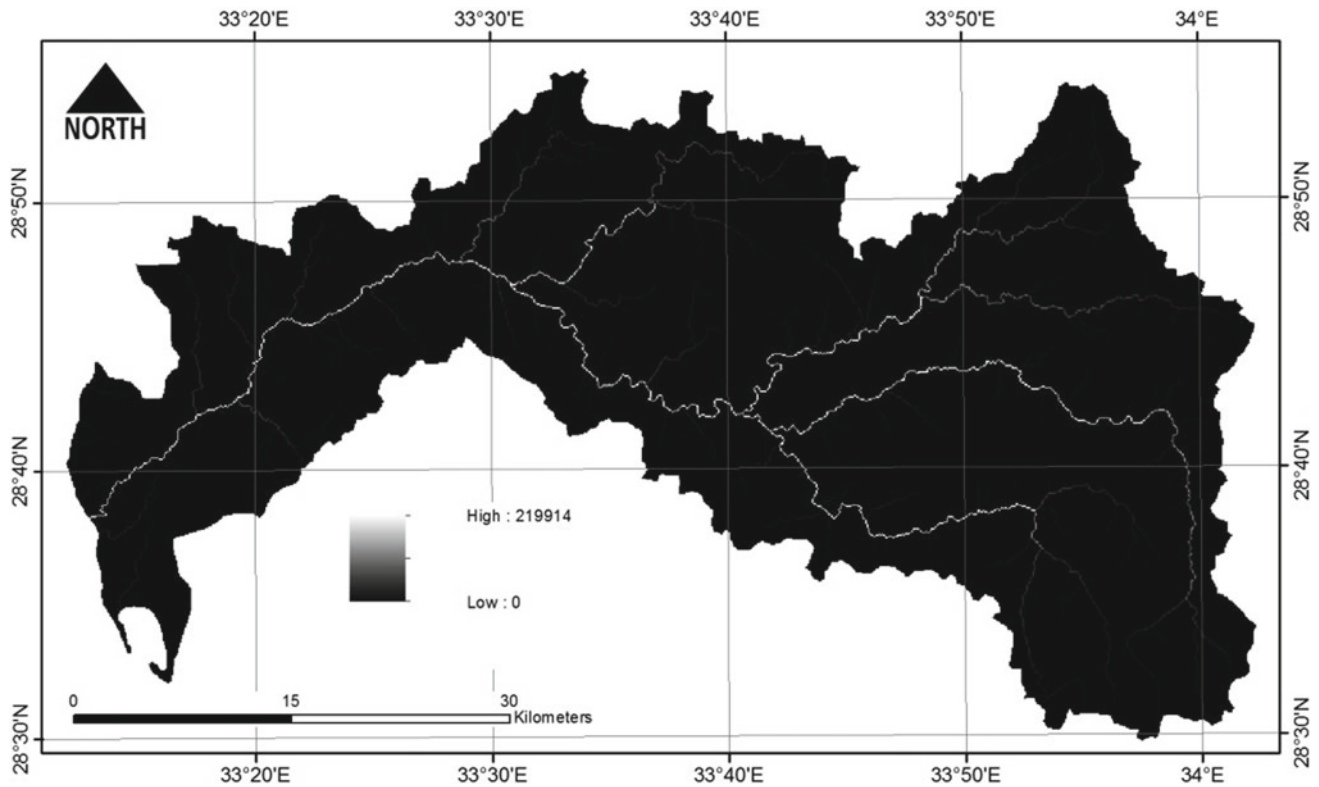

Fig. 7 Flow accumulation in the study area

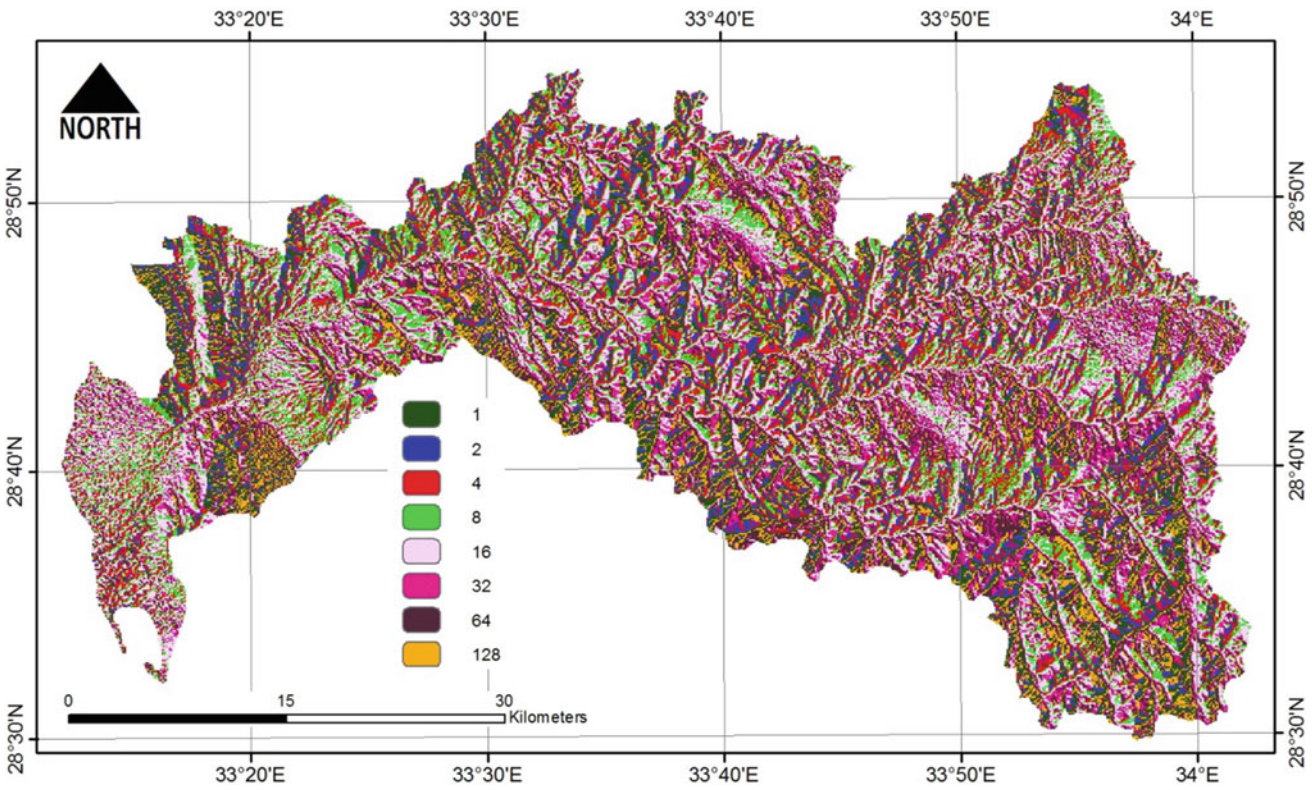

Fig. 8 Flow directions in the study area

infiltrometer using the formula developed by Philip (1957) for calculations. Figures 12, 13, 14 and 15 show infiltration rate curves and Table 3 infiltration rate values at the Wadi Hashim watershed.

3.2.4 Hydrological Soil Groups

Using soil texture and infiltration rates the Wadi Hashim watershed was broken down into three hydrological soil groups (HSGs) (according to USDA): A, C, and D (Table 4 and Fig. 16). The results show that HSG A is dominant, with 55.5% coverage, followed by type C and type D with coverages of 36.8% and 7.7% respectively.

3.3 The Depth and Volume of Runoff

Curve numbers (CNs) for different land uses in the watershed were obtained according to land use classes and HSGs (Fig. 17), from which were calculated the composite curve number (CNc) of the watershed and the runoff depth, as previous detailed. The rainfall and runoff volumes were obtained by multiplying the watershed area by the depth of rainfall and runoff with annual results generated from monthly results. Figure 18 shows the relationship between runoff and rainfall. Table 5 and Figs. 19 and 20 show annual rainfall and runoff volumes over 17 seasons and Fig. 21 compares average rainfall, runoff, and infiltration/evaporation at the Wadi Hashim watershed.

The results show that the relationship between rainfall and runoff at the Wadi Hashim watershed is linear with a correlation coefficient (R) of 0.9227. The Wadi Hashim watershed receives an average annual rainfall of 336,616 m^3. Of this, 56314 m^3 (16.7%) runs over the surface with the remainder, 280,302 m^3 (83.3%), undergoing infiltration or evaporation. Maximum rainfall occurred during the 2011/2012 season with a volume of 545,821 m^3; minimum was during the 2009/2010 season with a volume of 140,463 m^3. Maximum runoff was in the 2011/2012 season, with a volume of 138,452 m^3; minimum was in the 2009/2010 season, with a volume of 3359 m^3.

Based on runoff estimation, Fig. 22 shows the proposed location of a dam to prevent flood risk in this area.

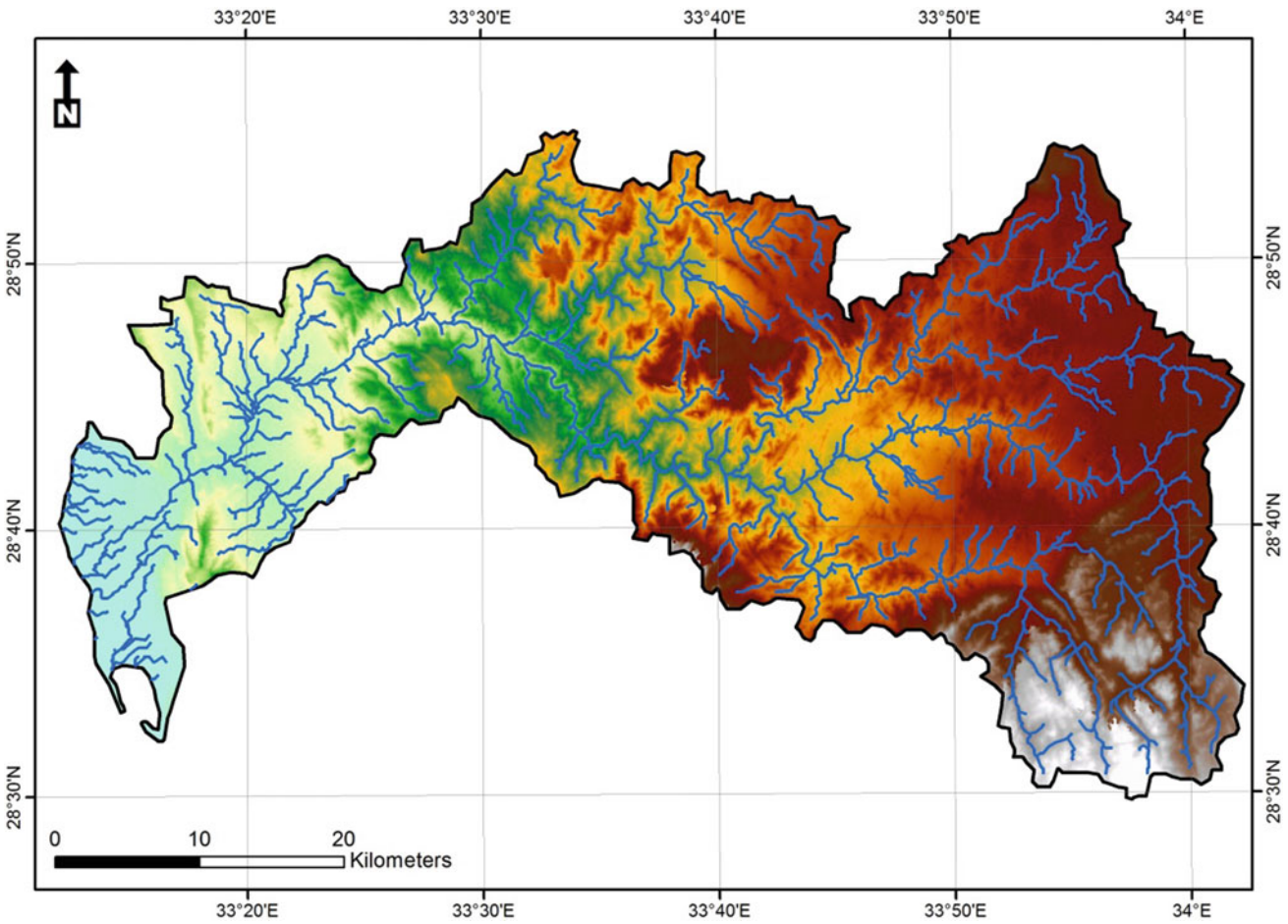

Fig. 9 Flood mapping in the Firan catchment and drainage area

4 Conclusions

This chapter demonstrates how remote-sensing techniques and GIS technology can be used effectively to extract a watershed and monitor flash flooding. Drainage flow directions, (upslope) areas, and catchments were extracted from DEMs in areas that have suffered flash flooding. Areas at risk of flooding were delineated. Such methodologies were applied to case studies in the Firan catchment, Sinai, and Wadi Hashim on the northern coast of Egypt.

In this study the GIS-based SCS-CN method was used to estimate runoff from the watershed. It is reasonable to conclude that land use planning and watershed management can effectively and efficiently be completed using the SCS-CN method and GIS. The study demonstrates that the combination of SCS-CN method and GIS is a powerful tool for estimating the runoff of ungauged watersheds, facilitating better watershed management and conservation. The methodology followed in this study can be applied to all wadi watersheds, but runoff and rainfall percentages will depend on watershed area and physical characteristics.

Our results suggest that the following would be beneficial:

1. Installing meteorological stations in all watersheds to provide spatial and temporal rainfall data that can be used for hydrological modeling.
2. Carrying out field measurements of runoff volumes at as many positions as possible and comparing results with the estimated values so that the SCS-CN method can be calibrated.

The results indicate that accurate watershed analysis can be developed successfully using remotely sensed data and currently available open source software. This approach saves time, effort, and cost. Finally, validation of the current technologies for watershed modeling and flash flood mapping is required through further research.

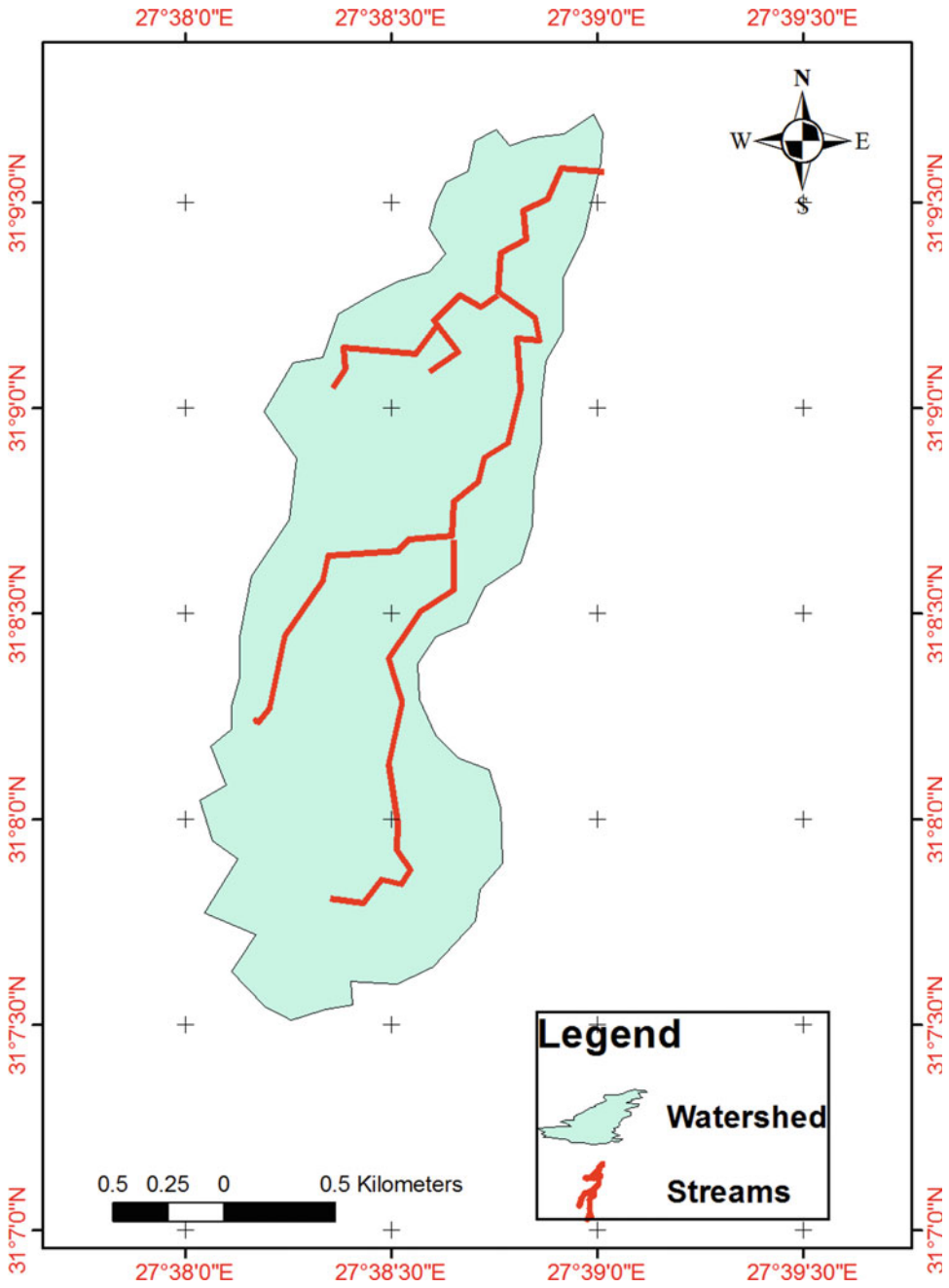

Fig. 10 The drainage networks and watershed of Wadi Hashim

Table 1 Classes of land use in the Wadi Hashim watershed

Land use	Area (m^2)	Percentage of area
1. Rock covered with thin hard crust	1.216	36.8
3. Cultivated area	0.255	7.7
3. Bare soil	1.834	55.5
Total	3.305	100

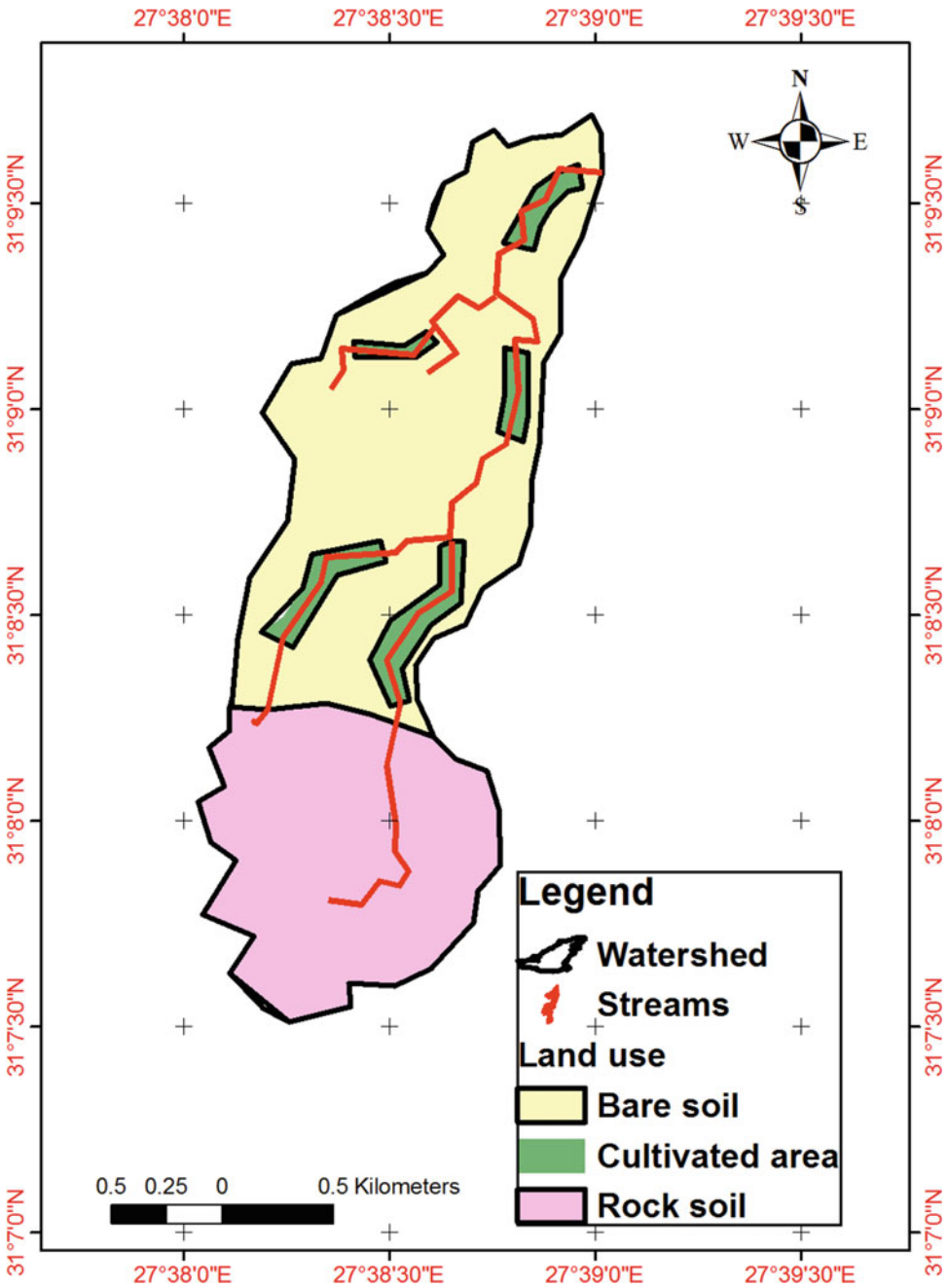

Fig. 11 Land use in the Wadi Hashim watershed

Table 2 Particle size distribution and soil textures from the Wadi Hashim watershed

Sample no.	Depth (cm)	Particles size distribution			Soil texture
		Sand (%)	Silt (%)	Clay (%)	
1	0–25	74.93	12.33	12.74	Sandy loam
	25–50	83.68	9.2	7.12	Sandy loam
2	0–25	73.41	18.5	8.09	Sandy loam
	25–50	80.26	14.28	5.46	Sandy loam
3	0–25	73.09	10.26	16.65	Sandy loam
	25–50	76.32	12.54	11.14	Sandy loam
4	0–25	78.03	15.26	6.71	Sandy loam
	25–50	78.87	11.9	9.23	Sandy loam

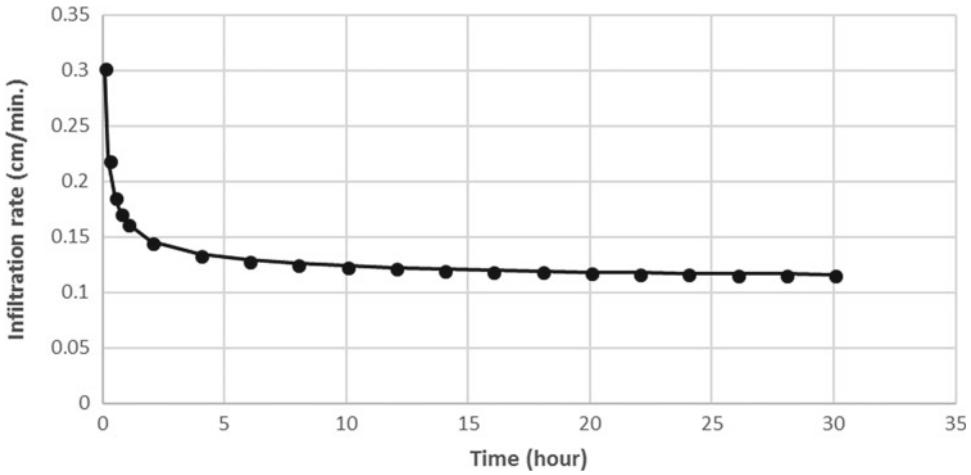

Fig. 12 Soil infiltration rate curve for Test 1

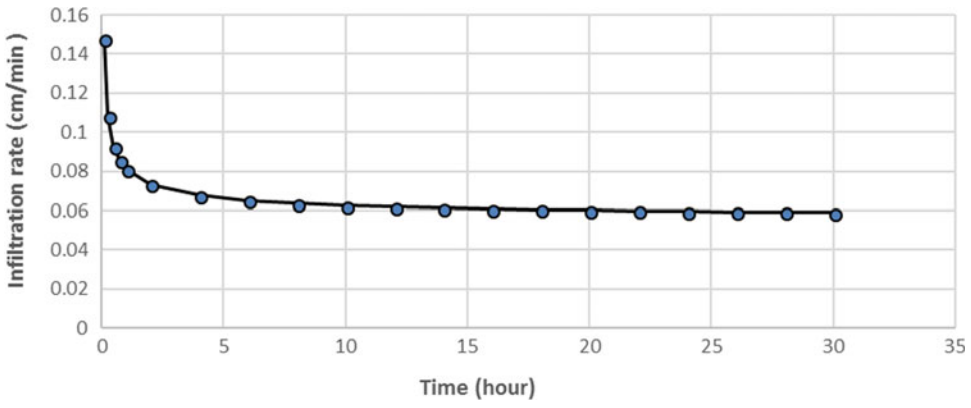

Fig. 13 Soil infiltration rate curve for Test 2

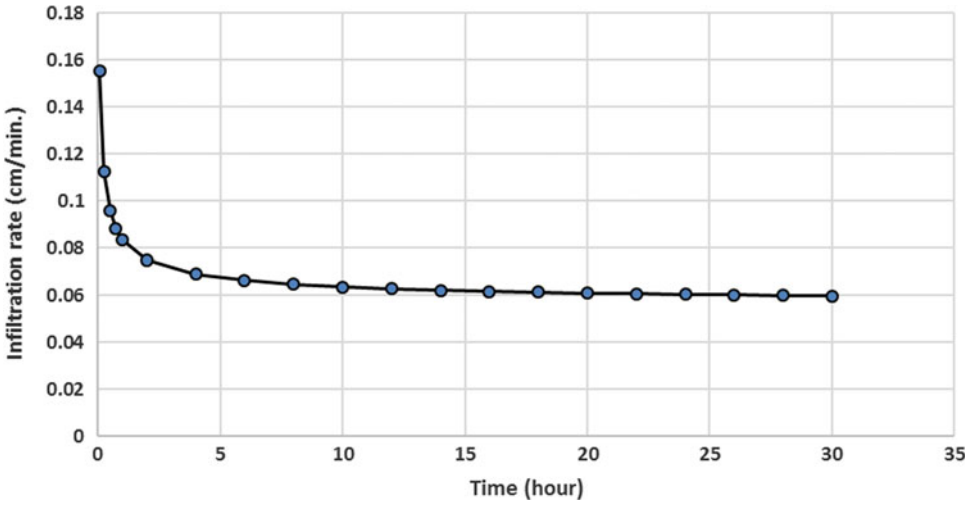

Fig. 14 Soil infiltration rate curve for Test 3

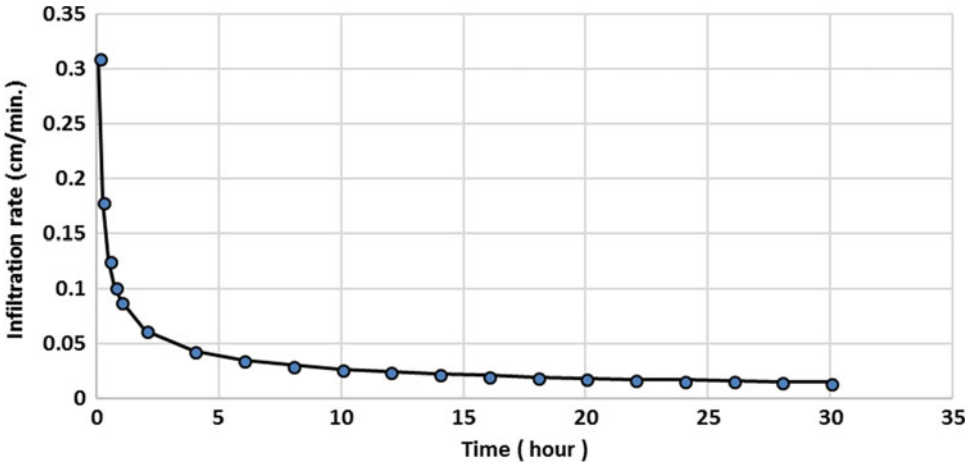

Fig. 15 Soil infiltration rate curve for Test 4

Table 3 Soil infiltration rates at different sites in the Wadi Hashim watershed

Test no.	Infiltration rate (cm/min)
1	0.12
2	0.06
3	0.06
4	0.02

Table 4 Hydrological soil groups at the Wadi Hashim watershed

Land cover	HSG	Area (km^2)	Percentage of area
1. Rock covered with thin hard crust	C	1.216	36.8
2. Cultivated area	D	0.255	7.7
3. Bare soil	A	1.834	55.5
Total		3.305	100

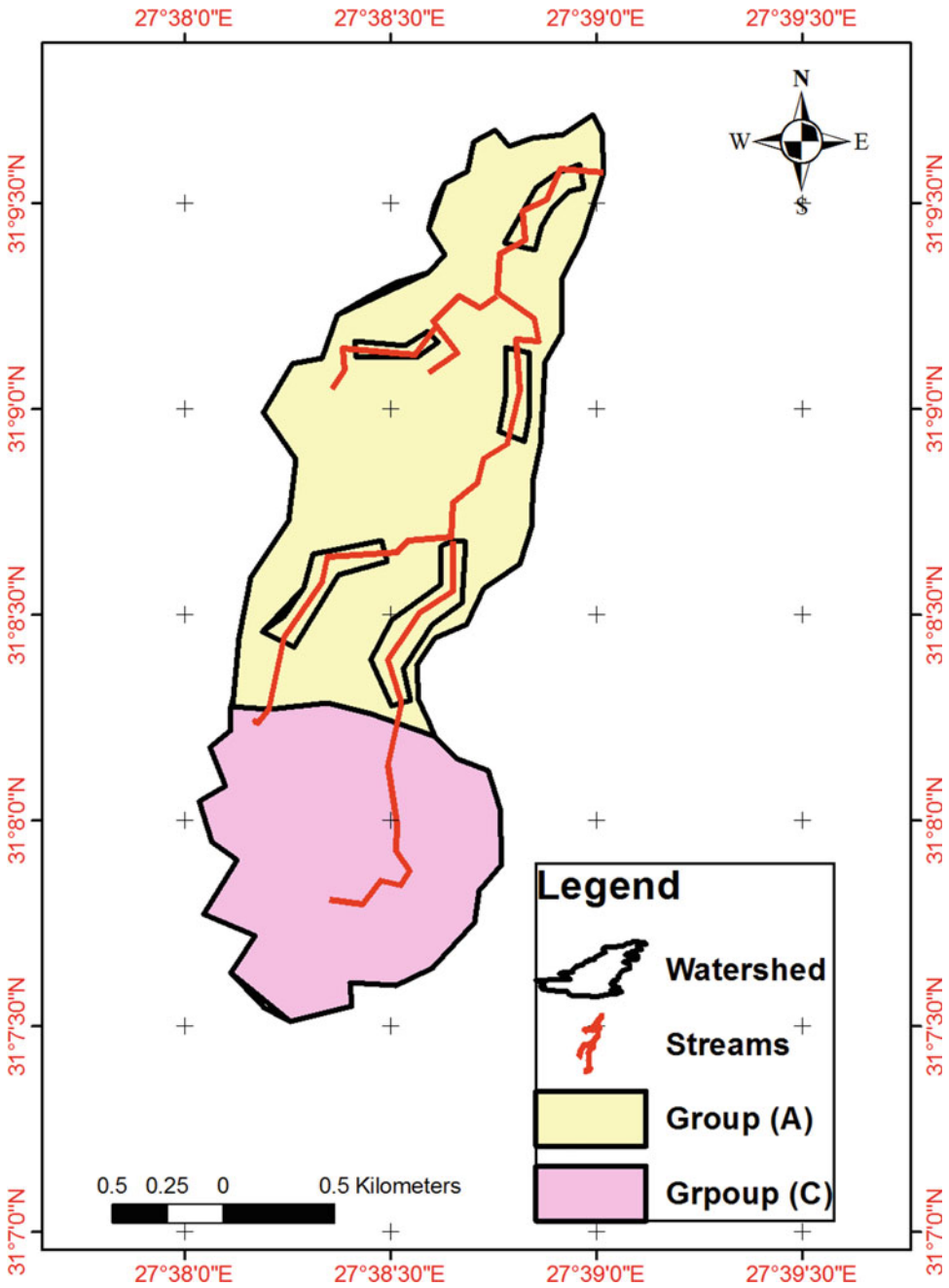

Fig. 16 Hydrological soil groups at the Wadi Hashim watershed

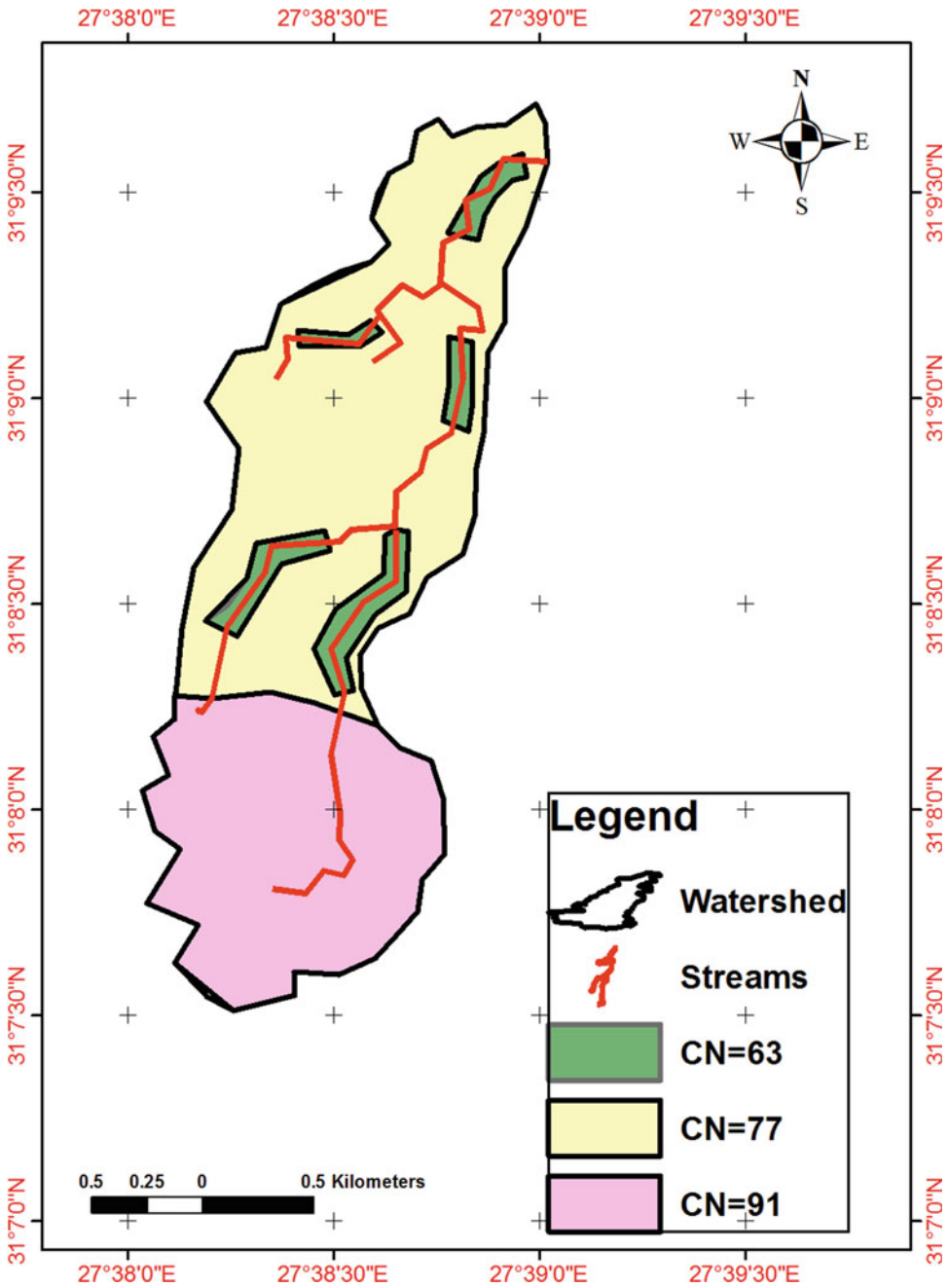

Fig. 17 Land use curve numbers (CN) at the Wadi Hashim watershed

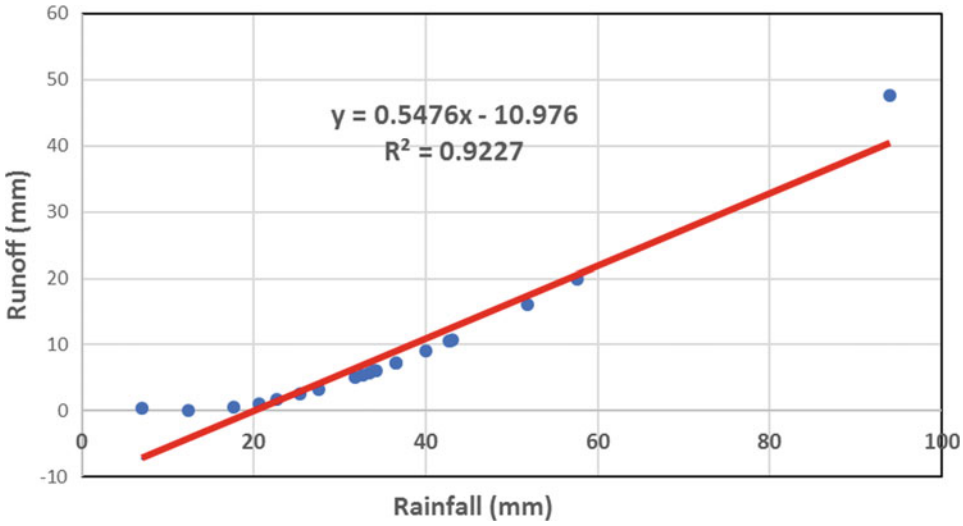

Fig. 18 Relationship between runoff and rainfall at the Wadi Hashim watershed

Table 5 Annual rainfall and runoff volumes over 17 seasons

Rainfall			Runoff	
Season	Depth (mm)	Volume (m^3)	Depth (mm)	Volume (m^3)
1998/1999	97.95	323,724.8	18.18	60,083.2
1999/2000	141.32	467,062.6	48.61	160,667.8
2000/2001	94.2	311,331	14.39	47,559.77
2001/2002	43.35	143,271.8	5.42	17,926.15
2002/2003	109	360,245	19.68	65,026.24
2003/2004	91	300,755	13.14	43,433.72
2004/2005	122	403,210	20.79	68,713.86
2005/2006	113.2	374,126	17.42	57,583.84
2006/2007	140.1	463,030.5	19.79	65,417.94
2007/2008	132	436,260	28.92	95,569.93
2008/2009	82.5	272,662.5	8.12	26,838.4
2009/2010	42.5	140,462.5	1.02	3,358.732
2010/2011	73.72	243,644.6	2.39	7,907.296
2011/2012	165.15	545,820.8	41.89	138,451.8
2012/2013	86.01	284,263.1	11.01	36,380.26
2013/2014	103.59	342,365	16.53	54,622.61
2014/2015	93.87	310,240.4	2.36	7,800.101
Total	1731.46	5,722,475	289.66	957,341.7
Average	101.8506	336,616.2	17.04	56,314.22

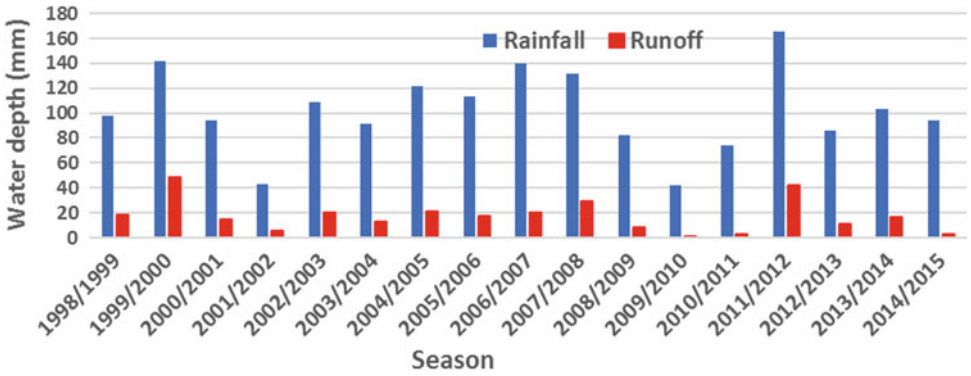

Fig. 19 Annual rainfall and runoff depths at the Wadi Hashim watershed for 17 seasons

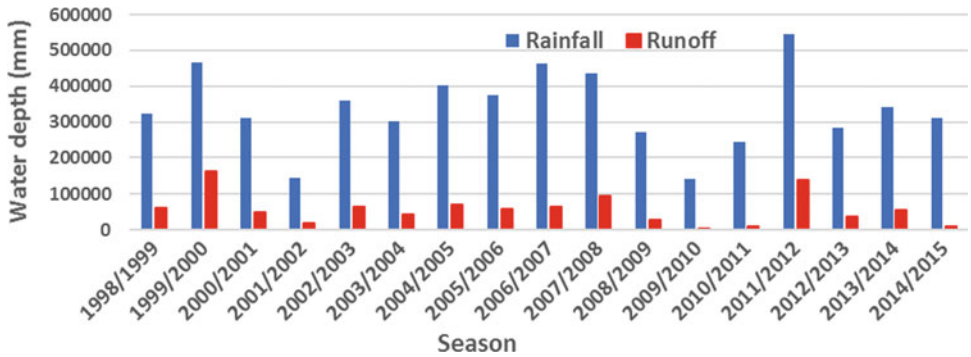

Fig. 20 Annual rainfall and runoff volumes at the Wadi Hashim watershed for 17 seasons

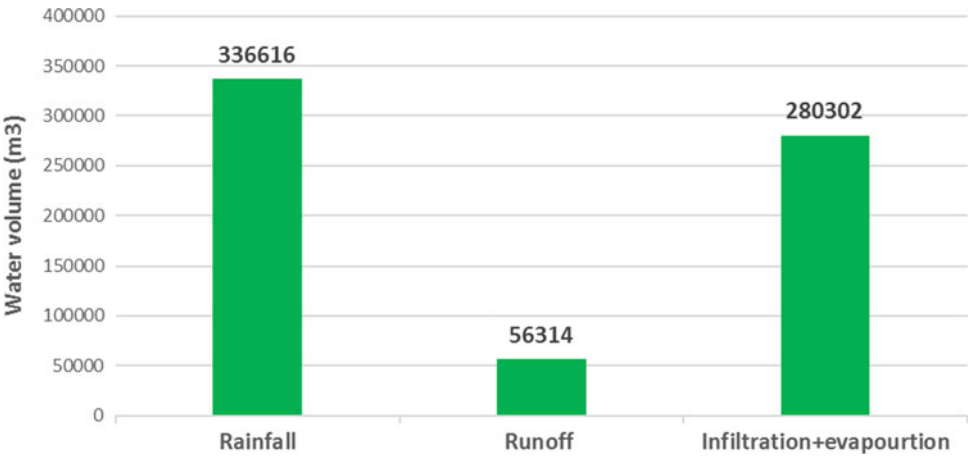

Fig. 21 Average rainfall, runoff, and infiltration/evaporation at the Wadi Hashim watershed

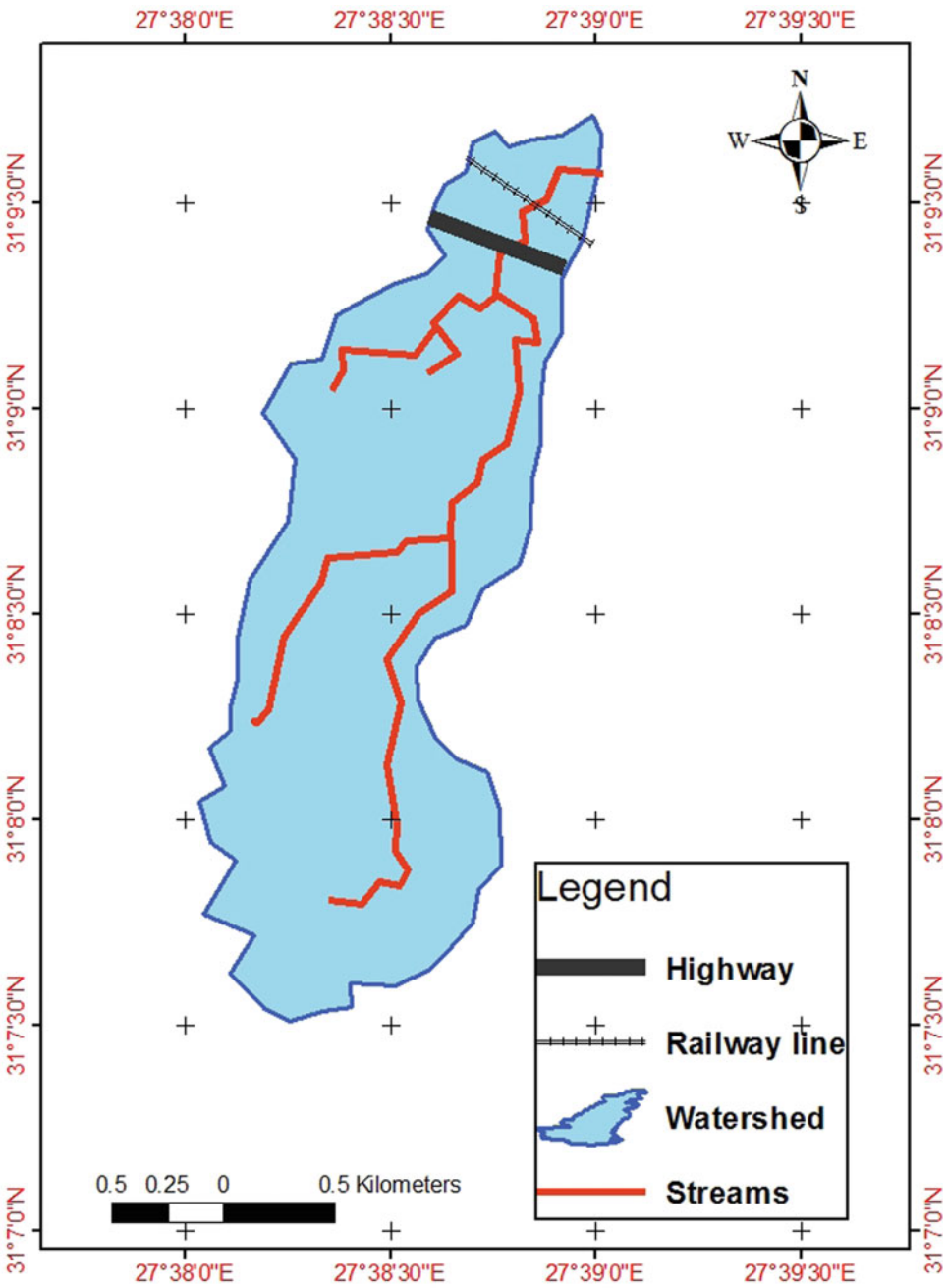

Fig. 22 Proposed location for a dam in the study area

References

AL-Gamdi, S. (1991). Estimating runoff curve numbers of the soil conservation service in arid and semi-arid environments using remotely sensed data. A dissertation Submitted to the Faculty of the University of Utah, USA.

Al-Jabari, S., Sharkh, A. M., & Al-Mimi, Z. (2009). Estimation of runoff for agricultural watershed using SCS curve number and GIS. In *Thirteenth International Water Technology Conference, IWTC 13 Hurghada*, Egypt.

Bansode, A., Patil, A. K. (2014). Estimation of runoff by using SCS curve number method and Arc GIS. *International Journal of Scientific & Engineering Research*, *5*. ISSN 2229-5518.

El Bastawesy, M., Ali, R. R., Nasr, A. H. (2008). The use of remote sensing and GIS for catchments delineation in Northwester Coast of Egypt: an assessment of water resources and soil potential. The *Egyptian Journal of Remote Sensing* and *Space* Sciences, *11*, 3–16.

El Bastawesy, M., White, K., & Nasr, A. (2009). Integration of remote sensing and GIS for modelling flash floods in Wadi Hudain catchment. *The Egyptian Hydrological Processes*, *23*, 1359–1368.

El Bastawesy, M., El Harby, K., & Habeebullah, T. (2012). The hydrology of Wadi Ibrahim Catchment in Makkah City, the Kingdom of Saudi Arabia: The interplay of urban development and flash flood Hazards. *Life Science Journal, in an Arid Environment. Journal of Hydrology*, *292*, 48–58.

ESRI. (2010). *Environmental systems research institute (ESRI) Press*. Redlands, California.

Jones, R. (2002). Algorithms for using a DEM for mapping catchment areas of stream sediment samples. *Computers & Geosciences 28*, 1051–1060.

O'Callaghan, J. F., & Mark, D. M. (1984). The extraction of drainage networks from digital elevation data. In *Computer vision, graphics and image processing* (Vol. 28, 323–344).

Philip, J. R. (1957). The theory of infiltration. 2–4 Soil Science, p. 34, 83, 85,163 and 257, 28.

Rashash Ali, A., Mohamed, E. S., Belal, A., El Shirbeny, M. (2015). GIS spatial model based for DAM reservoir on dry Wadis ACRS 2015. In *36th Asian Conference on Remote Sensing: Fostering Resilient Growth in Asia, Proceedings*.

Yousif, M., Abd, E. S. E., & Baraka, A. (2013). Assessment of water resources in some drainage basins, northwestern coast, Egypt. *35TApplied Water Science35T*, *3*, 35TI. 235T, pp. 439–452.